Pflügers Arch – Eur J Physiol (1995) 431: 186–195

ORIGINAL ARTICLE

Chinfei Chen · Stephen C. Cannon

Modulation of Na^+ channel inactivation by the β_1 subunit: a deletion analysis

Received: 23 May 1995/Received after revision: 14 August 1995/Accepted: 17 August 1995

Abstract Na^+ currents recorded from *Xenopus* oocytes expressing the Na^+ channel α subunit alone inactivate with two exponential components. The slow component predominates in monomeric channels, while co-expression with the β_1 subunit favors the fast component. Macropatch recordings show that the relative rates of these components are much greater than previously estimated from two-electrode measurements ($\approx$30-fold vs $\approx$5-fold). A re-assessment of steady-state inactivation, $h_\infty(V)$, shows that there is no depolarized shift of the slow component, provided a sufficiently long prepulse duration and repetition interval are used to achieve steady-state entry and recovery from inactivation, respectively. Deletion mutagenesis of the β_1 subunit was used to define which regions of the subunit are required to modulate inactivation kinetics. The carboxy tail, comprising the entire predicted intracellular domain, can be deleted without a loss of activity; whereas small deletions in the extracellular amino domain or the signal peptide totally disrupt function.

Key words Sodium channel · Gating · β Subunit · *Xenopus* oocyte

Introduction

Na^+ channels in adult skeletal muscle are heterodimers comprised of a large pore-forming α subunit and a smaller non-covalently associated β_1 subunit (reviewed in [5]). The physiological role of the β_1 subunit has not been completely established. The best system in which to observe the effects of the β_1 subunit has been the *Xenopus* oocyte. Injection of messenger ribonucleic acid (mRNA) encoding the α subunit alone leads to the expression of a voltage-activated channel highly selective for Na^+ ions, but the current inactivates anomalously slowly [12]. Co-injection of mRNAs for both the α and β_1 subunits produces heteromeric Na^+ channels that inactivate rapidly [4, 9], similar to the time course of Na^+ currents recorded from mammalian skeletal muscle. Addition of the β_1 subunit also accelerates recovery from inactivation and induces a leftward (hyperpolarizing) shift in the voltage dependence of inactivation produced by conditioning prepulses of 100–500 ms. The Na^+ current density is also increased when both mRNAs are injected. The role of the β_1 subunit in native mammalian cells, however, is not readily apparent by extrapolation of the results obtained in oocytes. In mammalian cell lines, either stable or transient transfection of the α subunit complementary deoxyribonucleic acid (cDNA) alone directs the expression of Na^+ channels with rapid inactivation kinetics [19, 25]. The predominant effects of adding the β_1 subunit are an earlier appearance of functional channels in the plasma membrane and an increased peak current density. Although the influence of the β_1 subunit on Na^+ channel inactivation appears to be mild in mammalian cells, understanding the mechanism of this modulation has great physiological relevance. It has recently been established that even subtle alterations of inactivation, such as those caused by missense mutations of the α subunit, can disrupt skeletal muscle excitability sufficiently to cause myotonia (stiffness) or paralysis [3].

Deletion mutations were constructed in the β_1 cDNA to define which regions of the subunit are necessary for modulation of Na^+ channel inactivation in oocytes. In order to more fully evaluate the consequences of β_1 subunit mutations, we also extended previous observations on the effects of co-injection with wild-type β_1 mRNA by recording Na^+ currents from macropatches.

C. Chen · S. C. Cannon (✉)
Department of Neurology, EDR 413A, Massachusetts General Hospital, Boston, MA 02114, USA

S. C. Cannon
Department of Neurobiology, Harvard Medical School, Boston, MA 02114, USA

With the improved bandwidth of the patch technique, we found that the rate of Na^+ current inactivation had previously been underestimated for the heteromeric channels. Consequently, co-expression of the β_1 subunit produced a 30-fold acceleration of inactivation rate, much larger than previous estimates of 5-fold. Patch formation itself also modified gating of α subunits and caused a time-dependent irreversible shift to the fast inactivating mode. Functional assays of β_1 subunit mutations show that deletions in the amino terminus cause a total loss of activity, while the carboxy tail can be removed without any impairment of function. In view of present models of β_1 subunit insertion into the plasma membrane, these results imply that modulation of Na^+ channel inactivation does not occur by interaction of α and β_1 subunits at a cytoplasmic site.

Materials and methods

Mutagenesis and mRNA preparation

Deletion mutations were constructed in the human β_1 cDNA [16] by using an overlap extension technique based on polymerase chain reaction (PCR) [8]. In the first PCR, the amplimers consisted of a wild-type antisense primer and a mutagenic forward primer that was complementary to the regions on either side of the segment to be deleted. The PCR-generated fragment from this first reaction contained the deletion and was used as the antisense primer in the second round PCR which extended the fragment beyond a unique restriction site upstream from the deletion. This final product was cut and directionally ligated into unique sites within the β_1 cDNA in Bluescript II (Strategene). Mutations were verified by sequencing both strands of the entire PCR fragment and flanking ligation sites (ABI Model 373A). 5'-Capped messenger RNAs coding for the adult rat skeletal muscle α subunit (SkM1 or μ1; [24]) and the human β_1 subunit were generated by in vitro translation of linearized plasmids (Megascript kit, Ambion).

Oocyte expression

Xenopus laevis were anesthetized with ice and MS222 (Sigma), and oocytes were removed by laparotomy. Stage V and VI oocytes were defolliculated enzymatically with collagenase (1 mg/ml, Gibco) and injected with 50 nl mRNA at concentrations of 0.1 to 1 μg/μl. For expression of heteromeric Na^+ channels, a 1:5 mass ratio of α to β_1 mRNA was used. This excess of β_1 mRNA is well into the region of saturation for modification of Na^+ currents by co-expression of both subunits [4]. Oocytes were incubated for 2–3 days at 18°C in ND-96 [96 mM NaCl, 2 mM KCl, 1.8 mM $CaCl_2$, 1 mM $MgCl_2$ and 5 mM 4-(2-hydroxyethyl)-1-piperazineethanesulfonic acid (HEPES), pH 7.6] supplemented with pyruvate (2.5 mM) and gentamicin (50 μg/ml).

Electrophysiology

Na^+ currents were measured with both two-electrode and macropatch techniques at room temperature, 20–22°C. For two-electrode recordings, oocytes were bathed in a low Ca^{2+} (0.3 mM) ND-96 solution. Electrodes were fabricated with a patch-pipette puller and had resistances of 0.5 to 1 MΩ when filled with 3M KCl. Currents were measured with a Dagan TEV 200 clamp, filtered at 10 kHz and sampled at 20 kHz. For macropatch recordings, the vitelline membrane was removed mechanically after shrinking the oocyte in a hyperosmolar solution. Bluntly tapered patch-pipettes with large tips (> 10 μm) were fabricated on a multi-stage puller (Sutter), coated with Sylgard (Dow) and firepolished to a smooth bullet shape. Electrodes were filled with (in mM): 100 NaCl, 2 $CaCl_2$, 1 $MgCl_2$, and 10 HEPES, pH 7.6, and had uncompensated series resistances of < 1 MΩ. The bath contained (in mM): 100 KCl, 5 ethylenebis(oxonitrilo) tetraacetate (EGTA), 1 $MgCl_2$, 10 HEPES, pH 7.6. Recordings were made from both cell-attached and excised inside-out patches. Currents were filtered at 10 kHz, and sampled at 20–40 kHz. Whenever a slow inactivating component of the Na^+ current was present, a 20-s repetition interval was used to allow sufficient time for complete recovery from inactivation between depolarizing pulses.

Data analysis

All current traces are shown after digital subtraction of linear leak and capacitance currents. Time constants were estimated by using a simplex algorithm to fit model functions to the Na^+ current. Inactivation was characterized by fitting the decaying phase of macroscopic Na^+ currents by the sum of two exponentials plus a constant. The fast and slow time constants usually differed by more than an order of magnitude and were therefore easily resolved. As an index of activation, the rising phase of the Na^+ current was approximated as the cube of an exponential with a time constant, τ_m.

The voltage dependence of the activation and inactivation time constants was fit using the Hodgkin-Huxley formalism, $\tau = 1/(\alpha + \beta)$, where α and β are the forward and reverse rate constants which are functions of voltage. For activation, $\alpha >> \beta$ over the range of our measurements so that:

$$\tau_m(V) \approx 1/\alpha = (1/\alpha\max) \exp(-V/k_m) \quad (1).$$

Conversely, for inactivation, $\beta >> \alpha$ so that:

$$\tau_h(V) \approx 1/\beta = (1/\beta\max)\{1 + \exp[-V - V_b)/k_b]\} \quad (2),$$

where V is the membrane potential, V_b is the voltage at which τ_h is twice the minimum, and the k values indicate the steepness of the voltage dependence in millivolts per e-fold change. These relations provide a standardized method to summarize the data and compare the behavior of mutants to wild-type. A rigorous mechanistic interpretation is not intended.

Results

β_1 subunit modulation of Na^+ channel kinetics

Na^+ currents elicited by a series of depolarizations are shown in Fig. 1 for oocytes injected with α subunit mRNA alone (monomeric channels) or a 1:5 combination of α and β_1 mRNAs (heterodimeric channels). Similar to the observations with two-electrode recording [4, 9], currents recorded from cell-attached macropatches inactivated much more slowly for monomeric channels compared to α:β_1 heterodimers. For monomeric channels, the Na^+ current was not completely inactivated by the end of a 40-ms depolarization, whereas for α:β_1 dimers, the current inactivated within milliseconds and was undetectable after 5 ms (note the four fold difference in time scale for Figs. 1A

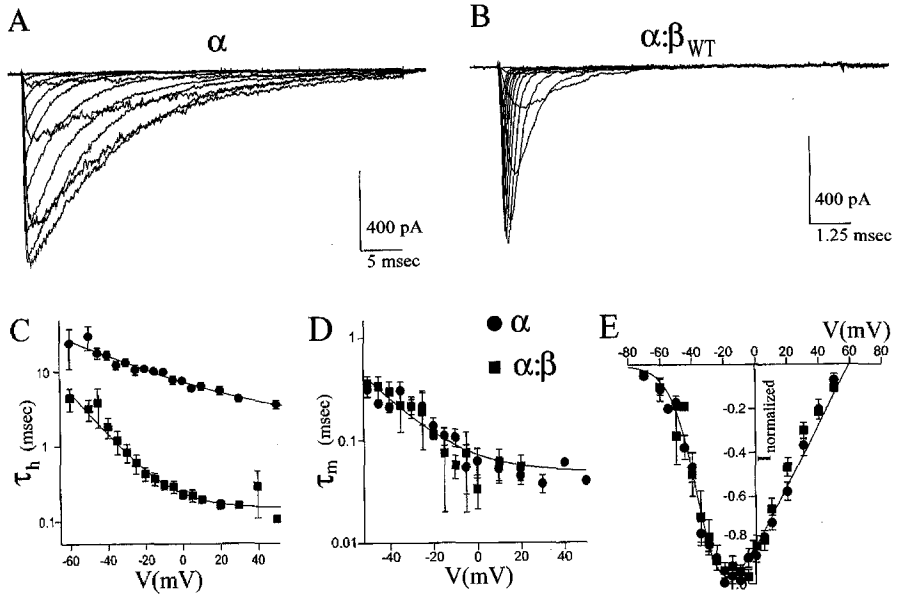

Fig. 1A–E The fast and slow modes of Na^+ current inactivation. Na^+ currents were recorded from macropathces on oocytes injected with mRNA encoding the α subunit (**A**) or the α and β_1 subunits (**B**). Currents were elicited from a holding potential of −120 mV by depolarizing to test potentials from −60 to 60 mV in 5- to 10-mV steps. The repetition interval was 20 s. **C** Macroscopic decay of the Na^+ current was fit to a two exponential decay, and the dominant time constant (τ_h), was plotted as a function of voltage for α (*circles*, $n = 10$) and $\alpha:\beta_1$ Na^+ channels (*squares*, $n = 9$). *Solid lines* represent theoretical fits for voltage dependence of τ_h [$\tau_h(V)$] as described in Materials and methods ($\alpha:\beta_1$: maximal reverse rate constant, $\beta_{max} = 6710\ s^{-1}$; voltage at which τ_h is twice the minimum, $V_b = -8.25$ mV; steepness $k_b = 14.6$ mV per e-fold change. $\alpha:\beta_{max} = 470\ s^{-1}$; $V_b = 34.1$ mV; $k_b = 38.8$ mV pere-fold change). **D** The kinetics of activation were comparable for $\alpha:\beta_1$ channels. Currents were fit by m^3h kinetics (from the model of Hodgkin and Huxley), and the activation parameter (τ_m) is plotted for α (*circles*, $n = 3$) and $\alpha:\beta_1$ (*squares*, $n = 7$) Na^+ channels. The sampling interval was decreased to 30 μs and the anti-aliasing filter cut-off set to 20 kHz for measurement of activation. *Solid lines* represent theoretical fits of τ_m ($\beta_{max} = 22{,}600\ s^{-1}$; $V_b = -15.5$ mV; $k_b = 12.0$ mV per e-fold change). **E** Normalized peak current/voltage (I/V) relationships of α (*circles*, $n = 10$) and $\alpha:\beta_1$ Na^+ channels (*squares*, n = 9) were identical. *Solid line* represents the best fit by an ohmic conductance with a voltage-dependent open probability that follows a Boltzmann distribution, $I = G_{max}(V - E_{rev}) \times \{[1 + \exp[-(V - V_a)/k]\}^{-1}$, where maximal conductance, $G_{max} = 0.014$, reversal potential $E_{rev} = 59.3$ mV, $V_a = -35$ and $k = 8.10$ mV

and B). Inactivation of the macroscopic Na^+ current was quantified by fitting the decay with the sum of two exponentials. For records similar to those in Figs. 1A, B, the vast majority of the decay was approximated well by one of the two exponentials. The voltage dependence of this larger predominant component, τ_h, is shown for data pooled from many cells in Fig. 1C. Inactivation was slower for monomeric channels at all voltages. At −10 mV, τ_h for monomeric Na^+ channels was 32 times larger than for heteromers. Furthermore, the asymptotic minima and the steepness of the voltage dependence of τ_h were different for the two channel types (α: 2.1 ms, 38.8 mV/e-fold; $\alpha:\beta_1$: 0.15 ms, 14.6 mV/e-fold). Thus the difference between the two forms of inactivation cannot be explained solely by a shift in the voltage dependence of gating.

The improved time resolution provided by the macropatch technique enabled us to compare the time course of activation for monomeric versus heteromeric Na^+ channels. The kinetics of activation were quantified by fitting the Na^+ current with the m^3h model of Hodgkin and Huxley (see Materials and methods). Figure 1D shows the voltage dependence of the activation parameter, τ_m, for oocytes injected with α or $\alpha:\beta_1$ mRNA. There was no detectable difference over a voltage range from −50 to + 20 mV. The peak current voltage (I/V) relationship also failed to reveal a difference in the voltage dependence of activation (Fig. 1E). Both channel types initially activated near −70 mV and had a maximal inward current at −20 mV. The reversal potential was greater than + 60 mV for either channel type which demonstrates that selectivity for Na^+ over K^+ was not altered by co-expression with the β_1 subunit.

Patch formation produced an irreversible shift to the fast inactivating mode

The patch-clamp technique improved the bandwidth of the voltage-clamp, but also caused a time-dependent shift in the kinetics of inactivation that did not occur with two-electrode recordings. The tracings in Fig. 1 show Na^+ currents recorded shortly after formation of a gigaohm seal. These data were selected because the current decay in each trial was approximated well by a single exponential which enabled a quantitative comparison between channel types to be made

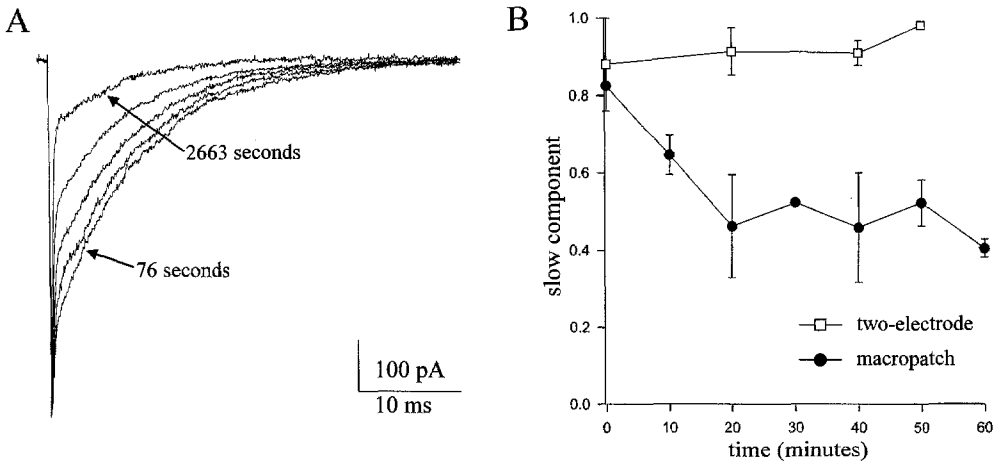

Fig. 2A,B Na^+ currents in macropatches shift irreversibly to the fast inactivating mode. **A** Superposition of amplitude-normalized Na^+ currents recorded over the lifetime of a single cell-attached macropatch. Patch durations: 76, 566, 911, 1240 and 2663 s. **B** The relative amplitude of the slow inactivating component is plotted as a function of recording time for macropatch (*circles*, $n = 5$) and two-electrode (*squares*, $n = 4$) measurements. The time values were binned into 10-min intervals

with a single parameter, τ_h. In most cell-attached macropatches (> 80%), however, the current conducted by monomeric Na^+ channels (α subunit only) inactivated with two distinct exponential components as shown in Figs. 2 and 3. The time constants of the slow and fast components, and their voltage dependence, were indistinguishable from values obtained in data sets with the monoexponential decays for either monomeric or heteromeric Na^+ channels. Thus the two phases of decay in Fig. 2 and 3 were produced by a linear combination of the same two inactivation patterns illustrated in Figs. 1A and B. The biexponential decay is the macroscopic correlate of the modal shift between fast and slow inactivation kinetics observed for unitary Na^+ currents [17, 26].

When the rat adult skeletal muscle isoform of the α subunit is expressed in *Xenopus* oocytes, the slow inactivating mode predominates for the unperturbed Na^+ channel. In recordings made with the two-electrode clamp, the gating behavior was stable over time, and 90% or more of the channels remained in the slow mode, as shown in Fig. 2B. A *reversible* shift to the fast inactivating mode can be induced with the two-electrode clamp by rapid application of depolarizing voltage pulses [26]. At −120 mV, recovery from inactivation occurs within milliseconds into the fast inactivating mode, whereas several seconds are required for return to the slow mode. To avoid this recovery-dependent shift in gating mode, long recovery periods of 20 s at −120 mV were used for all the stimulus protocols in this study.

In macropatch recordings, inactivation was more noticeably biexponential with a larger fast inactivating component. The relative proportion of the two modes was variable from patch to patch, even among patches from the same oocyte. Over the course of minutes, there was an *irreversible* shift to the fast mode. Figure 2A illustrates this phenomena by superimposing the Na^+ currents recorded from a single macropatch at various times over the course of 40 min. The Na^+ current at 76 s was comprised of approximately 80% slow and 20% fast inactivating current. Over time, the fast gating component increased while the slow component decreased such that at 2663 s, approximately 80% of the channels were in the fast mode and 20% remained in the slow mode. The trend toward the fast mode is shown for data pooled from five macropatches in Fig. 2B. Patch excision to an inside-out configuration often accelerated the shift to the fast mode. We never observed a spontaneous reversion back to the slow mode. A limited series of experiments failed to identify factors that modulated the gating shift. Pretreatment of intact oocytes with 8-bromo-adenosine 5′-cyclic monophosphate (cAMP) or application of reducing agents to excised patches (5 mM dithiothreitol) failed to prevent or reverse the shift to the fast mode.

Both recording techniques initially revealed slow inactivating kinetics in currents from monomeric Na^+ channels. Addition of the β_1 subunit biased Na^+ channel gating towards the other extreme, such that greater than 90% of the current displayed fast inactivating kinetics. The predominance of the fast mode was observed in both two-electrode and macropatch recordings from heteromeric Na^+ channels. Furthermore, with heteromeric channels there was no shift in gating mode over the duration of the recording. Therefore, despite the slow shift toward the fast mode, the initial observations from macropatch recordings provide an accurate measure of the integrity of the β_1 subunit.

Steady-state inactivation properties

The voltage dependence of steady-state inactivation, $h_\infty(V)$, has previously been reported to be shifted 10–20 mV to the right for channels gating in the slow mode [1, 4, 9]. Since τ_h was about 30-fold slower for the slow compared to the fast inactivating mode, and a failure to allow sufficient time to reach steady-state will shift $h_\infty(V)$ to the right, we applied variable duration

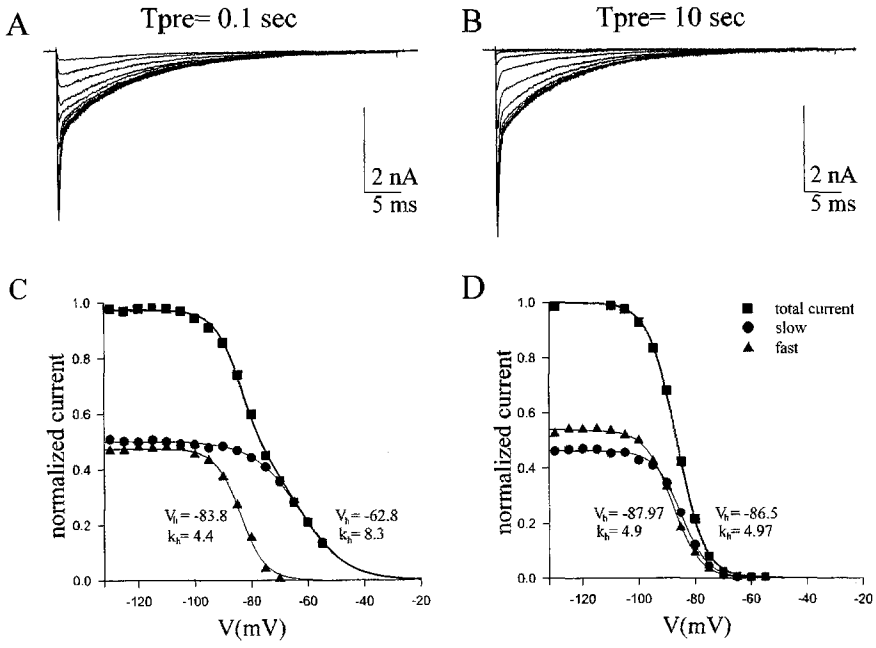

Fig. 3A–D Prepulse duration caused an apparent shift in the voltage dependence of steady-state inactivation. **A,B** Na^+ currents recorded from the same cell-attached macropatch on an oocyte injected with α subunit mRNA. Currents were elicited by a −10-mV test pulse after a prepulse of variable amplitude (−130 to −50 mV) was applied for: **A** 0.1 s or **B** 10 s; in both protocols the interval between trials was 20 s. Each response was fit with a sum of fast and slow inactivating components. The amplitude, normalized by the maximum current elicited from a prepulse of −130 mV, is shown for each component and the total current in **C** and **D**. The slow and fast inactivating components were each fit to a Boltzmann distribution, and the sum of the two fits is superimposed on the total current. With a short prepulse (**C**) there was an apparent depolarizing shift of the slow inactivating component, whereas with 10-s prepulses (**D**) the midpoints coincide for the rapid and slow components. (V_h voltage of half-maximal inactivation, K_h slope factor)

prepulses to test whether the shift in $h_\infty(V)$ for the slow mode is truly a steady-state property. Currents were recorded from macropatches on oocytes injected with α-subunit mRNA only. With this technique, steady-state inactivation properties could be measured in the same patch for both the fast and slow inactivating modes. Figure 3 shows families of Na^+ currents elicited by depolarization to −10 mV from prepulses of 0.1 or 10 s duration at potentials ranging from −120 to −55 mV. When a 0.1 s prepulse was used, the fast component inactivated at more negative prepulse potentials, leaving only the slow component at more depolarized potentials (Fig. 3A). In contrast, with a longer prepulse, both the fast and slow components decreased by the same proportion as more depolarized prepulses were applied (Fig. 3B).

The apparent shift in the voltage dependence of steady-state inactivation, caused by a prepulse of insufficient duration, is shown in Fig. 3C, D. The amplitudes of the slow and fast inactivating components were determined by fitting each trace with a two-exponential decay. The amplitudes of the slow (circles), fast (triangles), and total (squares) Na^+ currents were normalized by the total peak current elicited from a prepulse to −130 mV. For this particular patch, about half the Na^+ current inactivated rapidly and the other half gated in the slow mode. With a prepulse duration of 0.1 s, the relative availability of the slow mode appears to be shifted to the right of that for the fast mode, and the total current was fit best by the sum of two Boltzmann functions (Fig. 3C). Attempts to fit the total current in Fig. 3C with a single Boltzmann lead to the misinterpretation that the voltage dependence is less steep (larger k_h) for monomeric channels. When a longer prepulse duration was used for the same patch, however, there was no detectable difference in the voltage of half-maximal inactivation (V_h) or (k_h) slope factor between the fast and slow inactivating Na^+ currents (Fig. 3D). This phenomenon was reversible; returning to a shorter prepulse duration after testing with a 10 s prepulse caused the apparent shift of V_h to re-appear. Thus the shift in V_h was not caused by the progressive leftward shift in the voltage dependence of Na^+ channel gating that occurs irreversibly in dialyzed whole-cell or patch recordings [6]. In summary, despite the large difference in τ_h, steady-state inactivation was indistinguishable between the fast and slow gating modes of the Na^+ channel, provided a prepulse with a duration sufficiently long to achieve steady-state was applied.

Deletion mutations of the β_1 subunit

Site-directed deletions were made in the β_1 cDNA to localize functional domains of the subunit. In view of

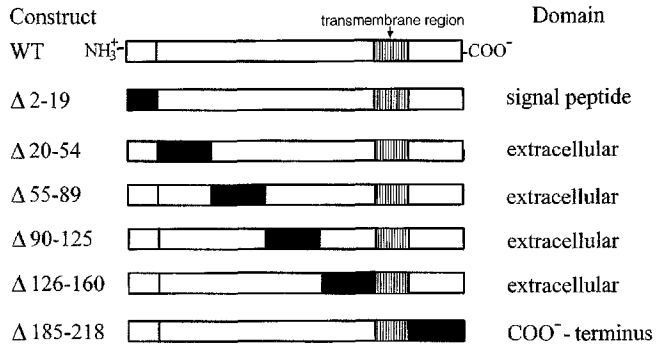

Fig. 4 Deletion mutations of the β_1 subunit. The membrane topology for the β_1 subunit is based on the model proposed by Isom and co-workers [9]. Deletion mutations (*shaded boxes*) were performed in the coding sequence for the signal peptide (Δ2–19), 25% of the extracellular domain (Δ20–54, Δ55–89, Δ90–125, Δ126–160), or the entire intracellular carboxy terminus (Δ185–218). No deletions were made in the transmembrane segment (*hatched lines*)

our re-examination of the β_1 subunit effects described above, the most reliable test for the presence of a normally functioning β_1 subunit is an increase in the probability that Na^+ channels gate in the fast inactivating mode. Based on the predicted membrane-folding structure of the protein [9], six deletion mutations were constructed in three separate domains of the 218 residue β_1 subunit: signal peptide, extracellular, and intracellular. Starting from the 5′-end of the cDNA, the first deletion, Δ2–19, removed the coding region of the signal peptide (Fig. 4). The remainder of the predicted extracellular segment was divided into four regions, each of which comprised a 35-residue deletion, Δ20–54, Δ55–89, Δ90–125, Δ126–160. No deletions were made in the putative membrane-spanning segment. The final deletion removed the entire intracellular carboxy terminus, Δ185–218. mRNAs from each of these constructs were co-injected with that of the skeletal muscle α subunit and screened with both two-electrode and macropatch measurements.

Removal of the entire intracellular domain did not produce a detectable change in β_1 subunit function. Figure 5A shows the Na^+ current recorded within 5 min of formation of a cell-attached macropatch on an oocyte co-injected with α and β_1 Δ185–218 mRNA. The entire Na^+ current inactivated rapidly. For every oocyte tested with either two-electrode (n = 7) or macropatch recording (n = 6), the α:β_1 Δ185–218 heterodimer gated in the fast inactivating mode (> 80% of the total current due to the fast component). Figure 5B shows a superposition of the best fits of $\tau_h(V)$ for wild-type monomeric or heteromeric channels with data from α:β_1 Δ185–218 mutants. The voltage dependence of τ_h for the intracellular deletion mutant closely matched that of α:β_1 wild-type channels. Therefore, β_1 subunit modulation of α subunit gating did not require the carboxy portion of the protein.

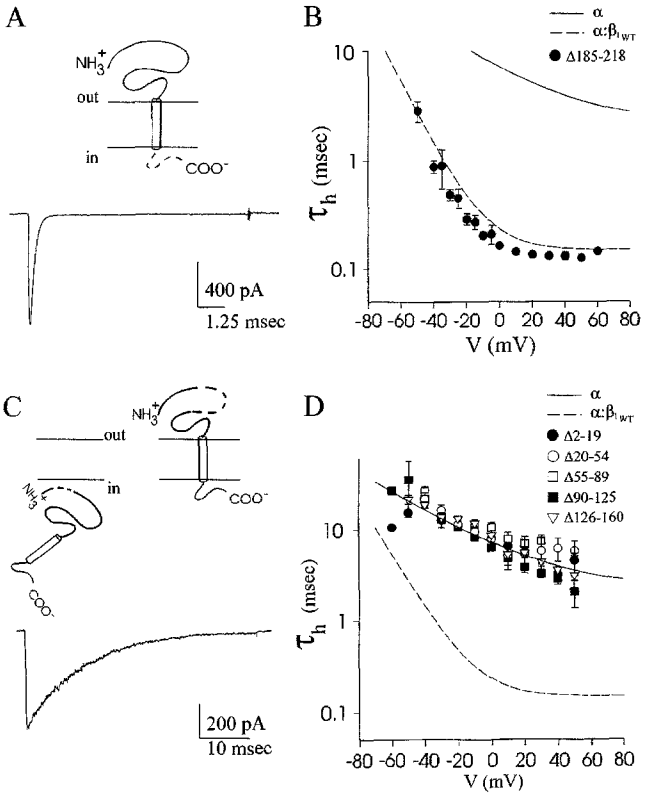

Fig. 5A–D Functional effects of β_1 subunit deletions. **A** Deletion of the carboxy terminus did not alter β_1 subunit function. Na^+ current was recorded from a macropatch depolarized to −10 mV from a holding potential of −120 mV. The fast inactivating mode predominated in this oocyte injected with a 1:5 ratio of mRNAs encoding α and β_1Δ185–218 subunits. *Inset* shows a stylized representation of the β_1 subunit with a carboxy deletion (*dashed line*). **B** The voltage dependence of τ_h [$\tau_h(V)$] for α:β_1 Δ185–218 channels was identical to that of α:β_1 wild-type, WT, channels (n = 6). **C** Amino terminus and single peptide deletions all caused a loss of β_1 function. Schematics illustrate possible fates of a β_1 subunit missing the single peptide or a portion of the extracellular domain (*dashed lines*). Trace shows the Na^+ current recorded from a macropatch containing α:β_1 Δ2–19 channels (signal peptide deleted). Similar responses were observed for all four amino deletion mutants. **D** For both signal peptide and amino terminus deletion mutants, the voltage dependence of τ_h matched that of monomeric Na^+ channels. (number of patches for Δ2–19 = 4, Δ20–54 = 3, Δ55–89 = 5, Δ90–125 = 4, Δ126–160 = 4). The *superimposed curves* are the fits of $\tau_h(V)$ for monomeric and α:β_1 WT dimeric Na^+ channels as shown in Fig. 1C

Deletions in the signal peptide or the putative extracellular domain all caused a loss of β_1 subunit function. Figure 5C shows the Na^+ current recorded from a macropatch on an oocyte injected with a 1:5 ratio of α and β_1 Δ2–19 mRNA, the signal peptide deletion. The slow inactivating mode dominated the decay of the Na^+ current. Similar results were obtained with each of the four extracellular deletion mutants: Δ20–54, Δ55–89, Δ90–126, and Δ126–160. The voltage dependence of τ_h for the signal peptide and extracellular deletion mutants paralleled that of monomeric Na^+ channels (Fig. 5D). Thus, in contrast to the carboxy

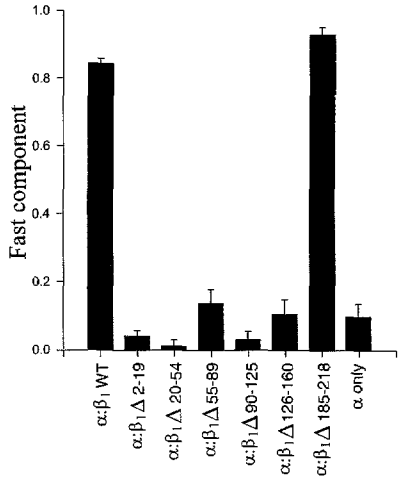

Fig. 6 Phenotype of the deletion mutations. The inactivating phase of Na^+ currents recorded with a two-electrode clamp was fit with a biexponential decay, and the ratio of the fast component to the total current is shown for each combination of mRNA injected (number of oocytes = 16 α:βWT; 9 Δ2–19; 8 Δ20–54; 9 Δ55–89; 5 Δ90–125; 14 Δ126–160; 7 Δ185–218; 8 α only)

terminal deletion, every deletion near the amino portion of the β_1 subunit caused a loss of its modulatory effect on α subunit gating.

The complete loss of β_1 subunit activity caused by deletion of the signal peptide or amino portions is more difficult to interpret. Possibilities include: protein synthesis was anomalously truncated, posttranslational processing was incomplete and thereby prevented trafficking and insertion into the plasma membrane, or even a properly oriented glycopeptide was non-functional. We suspect that deletion of the signal peptide blocked insertion into the plasma membrane. To experimentally determine the fate of the deletion mutants, and to further substantiate the proposed orientation of the β_1 subunit, we tried an immunohistochemical approach. The strategy was to insert an epitope tag at defined sites within the β_1 subunit cDNA, verify the functional integrity of the modified protein, and then probe for the location of the epitope with monoclonal antibodies. Coding sequences were inserted for either the hemagglutinin (single-letter code for amino acids YPYDVPDYA) or flag (DYKDDDDK) epitope at one of three sites: after the signal peptide, after E126 in the extracellular domain, or at the carboxy tail. Unfortunately, we were unable to detect any of the tagged β_1 subunits in either oocytes, transiently transfected HEK cells, or products of in vitro translation by immunohistochemical staining, Western blot, or immunoprecipitation. Functional assays of these insertion mutations, however, was consistent with effects produced by deletions. Insertion of either epitope at the amino terminus or in the extracellular domain (E126) caused a complete loss of β_1 modulation of inactivation, whereas the carboxy tag produced no functional change (data not shown).

Although the system bandwidth was superior with macropatch recordings, the two-electrode technique provided a better method for quantifying the fraction of the Na^+ current that resided in the fast or slow inactivating mode. The latter method was preferable because the two-electrode technique did not induce a shift in gating mode that occurred in macropatches (see Fig. 2). Figure 6 shows the proportion of the Na^+ current that inactivated in the fast mode for each of the combinations of mRNAs injected. The fast inactivating mode predominated only when the wild-type or the carboxy-deleted β_1 subunit mRNA was co-injected with α subunit mRNA. The slow mode predominated for all four deletions in the amino region of the β_1 subunit, and the distribution between the two modes was indistinguishable from the behavior of monomeric channels containing only the α subunit. Thus, in terms of the proposed structure of the β_1 subunit, the intracellular domain was not necessary for modulation of Na^+ channel inactivation, but deletion of the signal peptide or portions of the extracellular domain completely disrupt the effect of the β_1 subunit.

Discussion

Initially, we set out to identify regions of the β_1 subunit that are necessary for modulation of Na^+ channel gating in the oocyte, by use of deletion mutagenesis. To that end, it was concluded that 34 residues at the carboxy terminus can be deleted without a disruption of function, whereas deletions in the signal peptide or amino portion cause a total loss of function. In the process of optimizing the paradigm to assay the integrity of β_1 subunit function, we also gained a more complete understanding of the effects produced by co-expression of β_1 with the α subunit.

A re-investigation of β_1 subunit effects on Na^+ channel gating

Many of the new insights into β_1 subunit function were revealed by recording currents in macropatches rather than with a two-electrode clamp. The initial physiological characterization of β_1 subunit function [9] and subsequent studies that investigated the ability of the β_1 subunit to modulate gating in several isoforms of the α subunit [1, 4, 15, 18] all used the two-electrode voltage-clamp technique. In all of these reports, it was recognized that the ability to rapidly step the membrane potential is severely limited with two-electrode recording from oocytes, and therefore measurements of Na^+ channel activation were unreliable. However, it had not been appreciated that measurements of even the slower kinetics of inactivation may be distorted in two-electrode recordings. For Na^+ channels gating in

the fast inactivating mode, the measured time constant of macroscopic inactivation, τ_h, was artifactually large. Consequently, the relative difference in τ_h between the rapid and slow mode was previously underestimated. For the adult skeletal muscle isoform of the α subunit, SkM1, the Na^+ current elicited in macropatches by depolarization to -10 mV decayed 32-fold faster for heteromeric (α: β_1) than monomeric (α) channels. Two-electrode measurements revealed only a fivefold difference, primarily because estimates of τ_h for the fast mode were five- to sixfold too slow. In macropatch recordings of rat brain IIA (RBIIA) Na^+ channels expressed in oocytes, Fleig and colleagues [7] also observed a 25- to 30-fold difference between the fast and slow inactivating modes.

For monomeric SkM1 channels, Na^+ currents recorded from macropatches shifted irreversibly to the fast inactivating mode. The mode shift did not occur in two-electrode recordings. The same phenomenon has also been observed for RBIIA Na^+ channels [7]. Patch excision from oocytes also accelerates the rate of C-type inactivation in Kv1.3 K^+ channels. The on/off cell change does not occur with Kv1.6 K^+ channels, and chimeric substitutions showed that a single residue in the pore region, His 401 of Kv1.3, confers susceptibility to modulation by patch excision [14]. For Na^+ channels the mechanism of this mode shift remains to be established. Whatever the mechanism, this phenomenon may explain a long-standing discrepancy about the gating of Na^+ channels in the oocyte expression system. Several studies from Lester's laboratory showed that macroscopic inactivation of Na^+ channels comprised of the α subunit only was anomalously slow [12, 13]. Conversely, Stühmer's group observed fast inactivation kinetics for monomeric Na^+ channels [21, 22]. The difference may have arisen from the recording technique used. Stühmer's group recorded from macropatches while Lester's group used the two-electrode clamp.

Upon re-examination of inactivation properties of SkM1 in the oocyte expression system, we conclude that the voltage dependence of steady-state inactivation was not modulated by co-expression of the β_1 subunit. If a sufficiently long conditioning prepulse was applied, then there was no appreciable difference in the midpoint or the steepness of $h_\infty(V)$ for the fast and slow inactivating modes. For SkM1, sufficiently long meant 5–10 s. Krafte and colleagues [13] observed the same phenomenon with a slowly inactivating brain-derived α subunit, RBIIA. In their view, however, the reduction of the shift was produced by a kinetically distinct mechanism, slow inactivation. For Na^+ channels in skeletal muscle, however, slow inactivation equilibrates with a time constant of the order of several mintues [20]. The shift in V_h with prepulse duration in our experiments equilibrated in 10 s or less (see Fig. 3). Consequently, we do not interpret the shift in V_h as a reflection of a distinct slow or ultraslow inactivation process. Instead, we proposed that it occurs because the transition rates between closed and inactive conformations are slow for monomeric channels. Co-expression of the β_1 subunit accelerates the transition rates along this same pathway to inactivation from closed state(s) which enables the system to reach steady-state during even a 100-ms prepulse. The equilibrium distribution among these states, however, is not changed by the β_1 subunit. Therefore, when given sufficient time to reach *steady-state*, the voltage dependence of inactivation, $h_\infty(V)$, is the same for monomeric and heteromeric Na^+ channels.

A very different type of bimodal $h_\infty(V)$ was recently reported by Ji and co-workers [11]. In that study, Na^+ currents were recorded with two-electrode voltage-clamp measurements from oocytes injected with mRNA encoding SkM1. A portion of the channels were inactive at surprisingly negative prepulse potentials ($V_h = -130$ mV) when either depolarized holding potentials (-90 to -70 mV) or rapid application of pulses (repetition interval of 15 s or less) were applied. These voltage paradigms distort $h_\infty(V)$ because of insufficient time for full *recovery* from inactivation and should not be confused with the two components of $h_\infty(V)$ in Fig. 3C which arose from an insufficient time to allow *entry* to inactive state(s). In our view, the steady-state $h_\infty(V)$ is accurately measured only if long-duration prepulses (5 to10 s) are applied at a low repetition rate (once per 20 s or slower) from sufficiently hyperpolarized holding potentials (< -120 mV) to allow complete recovery from inactivation between trials.

A more controversial issue is whether co-expression of the β_1 subunit influences activation of the Na^+ channel. An analysis of activation was not possible (or over-intrepreted) in the majority of earlier studies due to the inability to step the membrane potential within a few hundred microseconds or less with the two-electrode clamp technique. Our macropatch recordings did not reveal an effect on activation of SkM1 by the β_1 subunit, as assessed by τ_m or the peak I/V relation. Fleig and colleagues [7] also found no significant difference in the activation time constant of the fast and slow modes in macropatch recordings of the RBIIA Na^+channel. Data from single-channel recordings have yielded conflicting results. Latency to first opening was prolonged for SkM1 [26], but not RBIII [17], for sweeps with bursts of openings (slow inactivating mode). Patton and colleagues [18] attempted to resolve the issue by co-expression of β_1 with a mutant α subunit that lacks fast inactivation. A slow component of macroscopic activation was reduced by co-expression of the β_1 subunit, but this component is only a minor portion (20–30%) of the total current. Thus, there is no established consensus on whether co-expression of the β_1 subunit modifies activation. All reports agree, however, that the effects on inactivation are much greater than any apparent change of activation.

Deletion mutagenesis shows the carboxy terminus of β_1 is non-essential

The extreme robustness of the β_1 effect made it feasible to use deletion mutagenesis to probe structure–function properties of the subunit. First, the modification of macroscopic inactivation produced by the β_1 subunit was readily detected. The time constant of the slow and fast inactivating modes differed by more than an order of magnitude which made the bi exponential fits unambiguous. Second, there was no overlap between monomeric channels and heterodimers in the relative amplitude of the slow and fast inactivating components (see Fig. 6). Third, expression of the β_1 effect was extremely consistent. In over 100 oocytes injected with α:β_1 wild-type mRNA, the fast inactivating mode predominated in every case; conversely the slow mode predominated in all oocytes injected with only α mRNA. Because of this robustness, we were confident in concluding that many deletions resulted in a complete functional loss of β_1 activity.

Our strongest conclusion from the deletion experiments is that the 34 residues at the carboxy terminal are not essential for β_1 function. This result was unexpected because this region is predicted to constitute the entire intracellular domain of the mature β_1 subunit [9], and rapid inactivation of Na^+ channels has been attributed to an intracellular domain of the α subunit, the III–IV cytoplasmic loop. The conformational changes in Na^+ channel structure that underlie the β_1 effect on inactivation apparently occur at transmembrane or extracellular sites of interaction between the subunits. There is precedence for modification of rapid inactivation from an extracellular site. Sea anemone and α-scorpion toxins impede inactivation when applied extra- but not intracellularly. Interestingly, both the β_1 subunit and the S5–S6 loop in domain I of the α subunit are labeled by photoactivatable derivatives of α-scorpion toxin [23]. Furthermore, such an external site may provide the mechanism by which an elevated extracellular K^+ concentration impedes inactivation in α subunit mutations that cause K^+-sensitive periodic paralysis [2]. Alternatively, the proposed topology of the β_1 subunit may be incorrect. Perhaps a portion of the amino terminal is intracellular. Such a drastic modification of the model seems unlikely, however, in view of established biochemical properties for the β_1 subunit (reviewed by Isom et al. [10]).

The deletion experiments also demonstrated that the gating changes induced by the β_1 subunit occurred as a collective set. None of the deletions produced dissociated changes in gating. For example, slowed entry to inactive state(s), as reflected by large $\tau_h(V)$, always occurred concomitantly with slowed recovery from inactivation. This behavior is consistent with the widely held view that the fast and slow modes are intrinsic properties of α subunit gating in the oocyte. The β_1 subunit biases the distribution between these endogenous modes, but does not create a new pathway for channel gating. Our data show that the mechanism of this modal bias does not require the terminal 34 residues of the β_1 subunit and therefore probably does not occur at an intracellular site.

Acknowledgements This work was supported by the Muscular Dystrophy Association, the National Institutes of Health (NIH) (AR42703), the Howard Hughes Medical Institute, and the Alfred P. Sloan Foundation. Adriana Pechanova assisted with RNA preparation and oocyte injections. We also thank David P. Corey, in whose laboratory many of the experiments were performed.

References

1. Bennett PB, Makita N, George AL (1993) A molecular basis for gating mode transitions in human skeletal muscle sodium channels. FEBS Lett 326:21–24
2. Cannon SC, Brown RH, Corey DP (1991) A sodium channel defect in hyperkalemic periodic paralysis: potassium-induced failure of inactivation. Neuron 6:619–626
3. Cannon SC, Brown RH, Corey DP (1993) Theoretical reconstruction of myotonia and paralysis caused by incomplete inactivation of sodium channels. Biophys J 65:270–288
4. Cannon SC, McClatchey AI, Gusella JF (1993) Modification of the Na current conducted by the rat skeletal muscle α subunit by co-expression with a human brain β subunit. Pflügers Arch 423:155–157
5. Catterall WA (1992) Cellular and molecular biology of voltage-gated sodium channels. Physiol Rev 72:S15–S48
6. Fernandez JM, Fox AP, Kranse S (1984) Membrane patches and whole-cell membranes: a comparison of electrical properties in rat clonal pituitary cells. J Physiol (Lond) 356:565–585
7. Fleig APCR, Rayner MD (1994) Kinetic mode switch of rat brain IIA Na channels in *Xenopus* oocytes excised macropatches. Pflügers Arch 427:399–405
8. Ho SN, Hunt HD, Horton RM, Pullen JK, Pease LR (1989) Site-directed mutagenesis by overlap extension using the polymerase chain reaction. Gene 77:55–59
9. Isom LL, DeJongh KS, Patton DE, Reber BFX, Offord J et al. (1992) Primary structure and functional expression of the β_1 subunit of the rat brain sodium channels. Science 256: 839–842
10. Isom LL, DeJongh KS, Catterall WA (1994) Auxiliary subunits of voltage-gated ion channels. Neuron 12:1183–1194
11. Ji S, Sun W, George AL, Horn R, Barchi RL (1994) Voltage-dependent regulation of modal gating in the rat SkM1 sodium channel expressed in *Xenopus* oocytes. J Gen Physiol 104:625–643
12. Krafte DS, Snutch TP, Leonard JP, Davidson N, Lester HA (1988) Evidence for the involvement of more than one mRNA species in controlling the inactivation process of rat and rabbit brain Na channels expressed in *Xenopus* oocytes. J Neurosci 8:2859–2868
13. Krafte DS, Goldin AL, Auld VJ, Dunn RJ, Davidson N, Lester H (1990) Inactivation of cloned Na channels expressed in *Xenopus* oocytes. J Gen Physiol 96:689–706
14. Kupper J, Bowlby MR, Marom S, Levitan IB (1995) Intracellular and extracellular amino acids that influence C-type inactivation and its modulation in a voltage-dependent potassium channel. Pflügers Arch 430:1–11
15. Makita N, Bennett PB, George AL (1994) Voltage-gated Na^+ channel β_1 subunit mRNA expressed in adult human skeletal muscle, heart, and brain is encoded by a single gene. J Biol Chem 269:7571–7578
16. McClatchey AI, Cannon SC, Slaugenhaupt SA, Gusella JF (1993) The cloning and expression of a sodium channel β_1-

subunit cDNA from human brain. Hum Mol Genet 2: 745–749
17. Moorman JR, Kirsch GE, VanDongen AMJ, Joho RH, Brown AM (1990) Fast and slow gating of sodium channels encoded by a single mRNA. Neuron 4:243–252
18. Patton DE, Isom LL, Catterall WA, Goldin AL (1994) The adult rat brain β_1 subunit modifies activation and inactivation gating of multiple sodium channel α subunits. J Bio Chem 269: 17649–17655
19. Scheuer T, Auld V, Boyd S, Offord J, Dunn R, Catterall WA (1990) Functional properties of rat brain sodium channels expressed in a somatic cell line. Science 247:854–858
20. Simoncini L, Stühmer W (1987) Slow sodium channel inactivation in rat fast-twitch muscle. J Physiol (Lond) 383:327–337
21. Stühmer W, Methfessel C, Sakmann B, Noda M, Numa S (1987) Patch clamp characterization of sodium channels expressed from rat brain cDNA. Eur Biophys J 14:131–138
22. Stühmer W, Conti F, Suzuki H, Wang X, Noda M et al. (1989) Structural parts involved in activation and inactivation of the sodium channel. Nature 339:597–603
23. Tejedor FJ, Catterall WA (1988) Site of covalent attachment of α-scorpion toxin derivatives in domain I of the sodium channel α subunit. Proc Natl Acad Sci USA 85:8742–8746
24. Trimmer JS, Cooperman SS, Tomiko SA, Zhou J, Crean SM et al. (1989) Primary structure and functional expression of a mammalian skeletal muscle sodium channel. Neuron 3: 33–49
25. Ukomadu C, Zhou J, Sigworth FJ, Agnew WS (1992) μ1 Na^+ channels expressed transiently in human embryonic kidney cells: biochemical and biophysical properties. Neuron 8:663–676
26. Zhou J, Potts JF, Trimmer JS, Agnew WS, Sigworth FJ (1991) Multiple gating modes and the effect of modulating factors on the μ1 sodium channel. Neuron 7:775–785